Fuel Cells

Deutsche Ausgabe: DOI: 10.1002/ange.201607118
Internationale Ausgabe: DOI: 10.1002/anie.201607118

Photoassisted Oxygen Reduction Reaction in H_2–O_2 Fuel Cells

*Bingqing Zhang, Shengyang Wang, Wenjun Fan, Weiguang Ma, Zhenxing Liang, Jingying Shi, Shijun Liao, and Can Li**

Abstract: *The oxygen reduction reaction (ORR) is a key step in H_2–O_2 fuel cells, which, however, suffers from slow kinetics even for state-of-the-art catalysts. In this work, by making use of photocatalysis, the ORR was significantly accelerated with a polymer semiconductor (polyterthiophene). The onset potential underwent a positive shift from 0.66 to 1.34 V, and the current was enhanced by a factor of 44 at 0.6 V. The improvement was further confirmed in a proof-of-concept light-driven H_2–O_2 fuel cell, in which the open circuit voltage (V_{oc}) increased from 0.64 to 1.18 V, and the short circuit current (J_{sc}) was doubled. This novel tandem structure combining a polymer solar cell and a fuel cell enables the simultaneous utilization of photo- and electrochemical energy, showing promising potential for applications in energy conversion and storage.*

The proton exchange membrane fuel cell (PEMFC) is a clean and efficient energy-conversion device with the potential to replace conventional fossil fuel combustion technologies. The oxygen reduction reaction (ORR) on the cathode is rather slow and thereby limits the performance of PEMFCs. Platinum is acknowledged to be the best catalyst for the ORR; however, its scarcity and high cost remain one of the greatest obstacles to the large-scale commercialization of PEMFCs.[1] To address this issue, enormous efforts have been devoted to developing novel catalytic materials, such as platinum alloys,[2] core–shell platinum catalysts,[3] and platinum-free heteroatom-doped carbon catalysts.[4]

Alternatively, other energy sources can be used to promote the ORR. For example, photoexcitation can tune the electron density distribution in a photocatalyst, which can improve the catalytic activity. In photocatalytic degradation, the oxidation of pollutants with O_2 is significantly accelerated as photogenerated electrons reduce molecular oxygen to strongly oxidizing species, such as H_2O_2 and O_2^-.[5] As such, it seemed feasible that photogenerated electrons may promote the complete reduction of oxygen to water. Winther-Jensen and co-workers[6] have reported that the activity of electrocatalytic ORR could be enhanced by illumination of two conjugated organic catalysts (PEDOT and polythiophene). Dong[7] and co-workers showed that light irradiation enhanced the performance of biofuel cells when using a photoresponsive cathode.

Herein, we describe that the ORR activity is greatly enhanced upon illumination of a polyterthiophene (pTTh) electrode. The onset potential was positively shifted from 0.66 to 1.34 V, and the current was enhanced by a factor of 44 at 0.6 V. A proof-of-concept light-driven H_2–O_2 fuel cell was then assembled; upon illumination, the V_{oc} increased from 0.64 to 1.18 V, and the J_{sc} value was doubled as well. These results show that photoassisted H_2–O_2 fuel cells can be considered as tandem structures combining a polymer solar cell and a conventional fuel cell.

Figure 1a shows that the onset potential of the ORR on pTTh is approximately 0.66 V (vs. RHE) in the dark. Upon light illumination, the onset potential is shifted to 1.34 V, which is much higher than that of a typical Pt/C catalyst (1.10 V) and the thermodynamic potential ($E^0 = 1.23$ V) of the ORR. The cathode current is $-1.2\ mA\,cm^{-2}$ at 0.6 V, which is 44 times higher than in the dark. Under these conditions, a negligible cathodic current was detected (see the Supporting Information, Figure S1) in argon-saturated solution. The above results strongly suggest that the kinetics of the ORR are considerably enhanced by the photocatalysis. To investigate the ORR mechanism on pTTh, we monitored the yield of peroxide species (HO_2^-) by rotating ring disc electrode (RRDE) measurements (Figure S2). Based on Equations S1 and S2, the H_2O_2 yield and electron transfer number were quantified with respect to the potential (Figure 1b). The H_2O_2 yield was about 100%, and the electron transfer number was about two over the entire potential range, indicating that the ORR on pTTh proceeds along a two-electron transfer pathway under illumination. The photoenhanced ORR activity was also confirmed in different electrolytes (see Figure S3).

Figure 2a shows a scanning electron microscopy (SEM) image of the pTTh film, which was synthesized by electropolymerization (see Figure S4 for the polymerization curves). The HR-SEM image in Figure 2b and the transmission electron microscopy (TEM) images in Figure 2c and d show the sheet-like morphology of pTTh. The thickness of the pTTh film was estimated to be approximately 3.0 μm according to a side-view SEM image (Figure S5). The UV/Vis absorption spectrum in Figure 2e shows that the pTTh film has a wide absorption range with the band edge at about 620 nm, which corresponds to the band gap of 2.0 eV. Cyclic

[*] Dr. B. Q. Zhang, Dr. S. Y. Wang, Dr. W. J. Fan, Dr. W. G. Ma, Prof. J. Y. Shi, Prof. C. Li
State Key Laboratory of Catalysis
Dalian National Laboratory for Clean Energy
Dalian Institute of Chemical Physics
Chinese Academy of Sciences
Dalian, Liaoning, 116023 (China)
E-mail: canli@dicp.ac.cn
Dr. B. Q. Zhang, Dr. W. J. Fan, Dr. Z. X. Liang, Prof. S. J. Liao
Key Laboratory of Fuel Cell Technology of Guangdong Province & Key Laboratory of New Energy Technology of Guangdong University
School of Chemistry and Chemical Engineering
South China University of Technology
Guangzhou, Guangdong, 510641 (China)

Supporting information for this article can be found under: http://dx.doi.org/10.1002/anie.201607118.

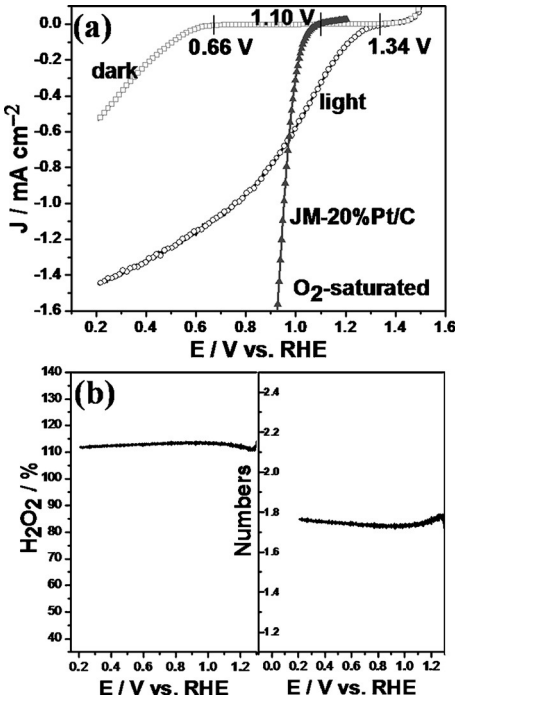

Figure 1. a) LSV curves of pTTh in O_2-saturated 0.10 M KOH electrolyte at a scan rate of 10 $mV s^{-1}$ and a rotation rate of 1600 rpm in the dark or under illumination; JM-20% Pt/C for comparison. b) The calculated production yields of H_2O_2 and the number of electrons transferred in the ORR according to a RRDE test at 1600 rpm under illumination. A xenon lamp was used as the light source, and the light intensity at the surface of the electrode was 300 $mW cm^{-2}$.

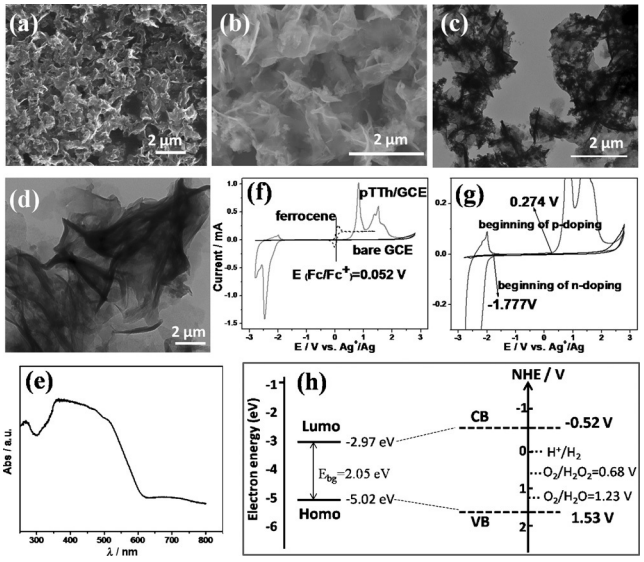

Figure 2. a) SEM image, b) HR-SEM image, c, d) TEM images, and e) UV/Vis absorption spectrum of a pTTh film. f) Cyclic voltammograms of pTTh/GCE in acetonitrile containing 0.10 M tetrabutylammonium hexafluorophosphate at a scan rate of 20 $mV s^{-1}$; the ferrocenium/ferrocene (Fc/Fc^+) redox potential was measured to calibrate the pseudo reference electrode (0.052 V vs. Ag in the present study). g) Enlarged image of the voltammogram in (f). h) Energy diagram showing the calculated HOMO and LUMO levels of pTTh in absolute vacuum energies and as potentials relative to the NHE.

voltammetry (CV) was performed to determine the energy levels of HOMO and LUMO, which correspond to the onset potentials of oxidation and reduction, respectively (Figure 2 f, g). The energy levels of HOMO and LUMO were calculated to be −5.02 eV and −2.97 eV, respectively (Figure 2 h) according to Equations S3 and S4, yielding an energy gap of 2.05 eV. The energy levels corresponding to the electrochemical potentials of the conduction band (CB) and valence band (VB, vs. NHE) are −0.52 V and 1.53 V, respectively.

A proof-of-concept light-driven H_2–O_2 fuel cell (Figure S6) was assembled with the pTTh/GCE cathode and a Pt/C anode to further confirm the photoenhancement effect. Figure 3 a shows that the V_{oc} value is 0.64 V in the dark and increased to 1.18 V upon illumination; for comparison, V_{oc} is 0.97 V for all Pt electrode based H_2–O_2 fuel cells (Figure S7). The J_{sc} and the maximum power density (P_{max}) of the illuminated H_2–O_2 fuel cell were 2.3 and 5.3 times larger than those in the dark. They were also higher than those of all Pt electrode based H_2–O_2 fuel cells at potentials above 0.9 V (Figure 3 b).

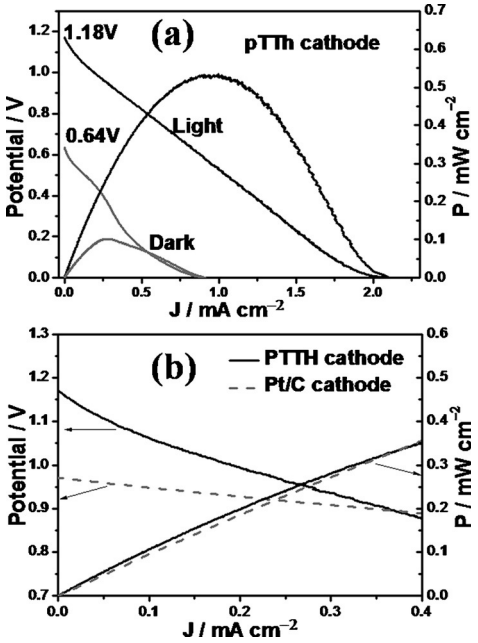

Figure 3. a) Performance of the proof-of-concept light-driven H_2–O_2 fuel cell featuring the pTTh photocathode. b) Comparing the performance of the pTTh-based fuel cell with H_2–O_2 fuel cells with Pt/C cathodes. A xenon lamp was used as the light source, and the light intensity at the surface of pTTh was 300 $mW cm^{-2}$.

In the dark, the fuel cell generates the electrochemical potential of the H_2–O_2 reaction. Under illumination, the polymer semiconductor absorbs light and generates electrons and holes, just as in the case of polymer solar cells. The difference between the light-driven H_2–O_2 fuel cell and a conventional polymer solar cell lies in the electron acceptor, which is O_2 in the former and fullerene in the latter. Even so, the increase in potential conferred by the illumination amounts to 0.68 and 0.54 V for the half-cell and fuel cell, respectively. This increase is similar to the photovoltage of

polymer solar cells, which typically lies in the range of 0.6–0.8 V.[8] The V_{oc} of the light-driven fuel cell roughly equals the sum of the electrochemical potential of the H_2–O_2 reaction and the photovoltage of the polymer solar cell. We therefore concluded that the light-driven fuel cell is a tandem device consisting of a fuel cell and a polymer solar cell, and a working diagram is presented in Figure 4a. The electrons generated by

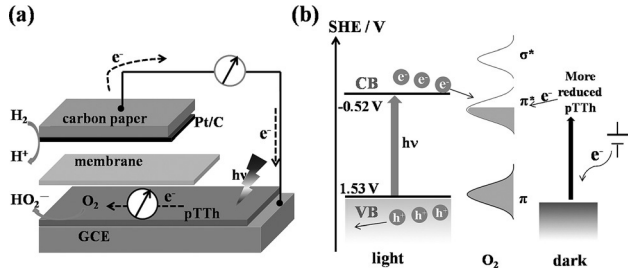

Figure 4. a) The working principle of the tandem cell. b) Schematic energy diagram for oxygen reduction on pTTh.

hydrogen oxidation on the anode side flow to the cathode side, yielding an electrochemical potential from the chemical reaction. At the cathode side, the semiconductor pTTh is excited and generates photovoltage upon illumination. As a result, photogenerated electrons are transferred to O_2 to promote its reduction, and the overall voltage results from both processes. The mechanism of the ORR on pTTh was proposed from the view of energy (see Figure 4b). In the dark, the Fermi level of pTTh is elevated as the applied bias is increased, and when the bias exceeds the electrochemical potential of the ORR, the electrons can be transferred from pTTh into the unoccupied π^*_{2p} orbitals of oxygen. Under illumination, electrons in the VB of pTTh are excited to the CB, and the resulting holes are transported to the anode via the external circuit. The excited electrons in the CB have sufficient potential to be transferred into the π^*_{2p} antibonding orbital of molecular oxygen, but may not be of sufficient energy for transfer into the σ* orbital. As a result, the ORR proceeds according to a two-electron transfer mechanism.

To further confirm the photoassistance effect, two monochromatic light sources were used to investigate the effect of the light wavelength and intensity on the ORR. Figure 5a shows that at the same light intensity, the performance is higher at an irradiation wavelength of 385 nm than at 580 nm. The onset potential is 120 mV more positive under 385 nm monochromatic light irradiation than under 580 nm irradiation, and the photocurrent is 2.9, 1.6, and 1.1 times higher than under 580 nm irradiation (1.23, 0.9, and 0.6 V, respectively; see Figure 5b). These results indicate that for the same number of photons, higher photon energies lead to a more positive onset potential. The performance of the ORR at different light intensities is analyzed in Figure 5c,d. The onset potential of the ORR remained constant at a given wavelength. The more positive onset potential under 385 nm than under 580 nm irradiation is consistent with the above result. The photocurrent increased with the light intensity for both 580 and 385 nm monochromatic light irradiation, revealing

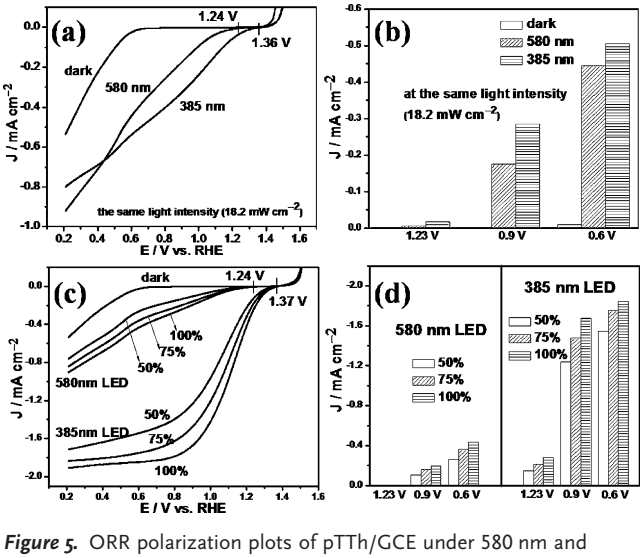

Figure 5. ORR polarization plots of pTTh/GCE under 580 nm and 385 nm monochromatic light irradiation with the same light intensity (a) and different light intensities (c). b,d) Current histograms of (a) and (c) at fixed potentials. LED-50%, -75%, and -100% are the light intensities of the monochromatic light; the light intensities at the surface of the electrode (the distance between light source and electrode is 5 cm) are as follows: 580 nm LED-50%: 9.7 mW cm^{-2}; 580 nm LED-75%: 14.3 mW cm^{-2}; 580 nm LED-100%: 18.2 mW cm^{-2}; 385 nm LED-50%: 102 mW cm^{-2}; 385 nm LED-75%: 164 mW cm^{-2}; 385 nm LED-100%: 224 mW cm^{-2}. The tests were conducted in O_2-saturated 0.10 M KOH electrolyte at a scan rate of 10 mV s^{-1} and a rotation rate of 1600 rpm.

that the ORR current is roughly proportional to the number of photogenerated electrons.

The stability of the ORR on pTTh cathode was investigated by a chronoamperometry test at 0.8 V under light illumination. The photocurrent remained unchanged in a 10 h test (Figure S8), indicating that the photocathode is quite stable in the presence of oxygen and illumination.

Finally, some other semiconductor polymers (P3HT, PCDTBT, PTB7, and PDPP3T), which are common donor materials in polymer solar cells, were also investigated for the photoassisted ORR. Their light absorption spectra are shown in Figure S9. Under illumination, the onset potentials of the ORRs on these polymers were significantly shifted in the positive direction, and the currents increased (Figure S10 and Table S1). These polymers were then used as the photocathodes in H_2–O_2 fuel cells, and a similar trend was seen as for pTTh: The V_{oc} increased by 0.33–0.77 V under illumination (Figure S11 and Table S2). These findings corroborate the general applicability of the tandem structure combining a fuel cell and a polymer solar cell.

In summary, we have shown that the ORR is significantly enhanced on polymer semiconductor photoelectrodes upon light irradiation, by combining electrocatalysis with photocatalysis. The onset potential of the ORR was shifted from 0.66 to 1.34 V upon illumination, and the current density increased by a factor of 44. This photoelectrode was then employed in a proof-of-concept light-driven H_2–O_2 fuel cell device; upon illumination, the cell V_{oc} increased from 0.64 to 1.18 V, and the J_{sc} value doubled. This novel design enables

the simultaneous utilization of photo- and electrochemical energy, yielding a superior performance.

Acknowledgements

This work was financially supported by the 973 National Basic Research Program of the Ministry of Science and Technology (2014CB239400) and by the National Natural Science Foundation of China (21090340).

Keywords: electrocatalysis · fuel cells · oxygen reduction reaction · photocatalysis · polymers

How to cite: *Angew. Chem. Int. Ed.* **2016**, *55*, 14748–14751
Angew. Chem. **2016**, *128*, 14968–14971

[1] a) E. Yeager, *Electrochim. Acta* **1984**, *29*, 1527–1537; b) N. Marković, T. Schmidt, V. Stamenković, P. Ross, *Fuel Cells* **2001**, *1*, 105–116; c) M. K. Debe, *Nature* **2012**, *486*, 43–51.

[2] a) V. Stamenković, B. S. Mun, K. J. J. Mayrhofer, P. N. Ross, N. M. Markovic, J. Rossmeisl, J. Greeley, J. K. Nørskov, *Angew. Chem. Int. Ed.* **2006**, *45*, 2897–2901; *Angew. Chem.* **2006**, *118*, 2963–2967; b) J. Greeley, I. E. L. Stephens, A. S. Bondarenko, T. P. Johansson, H. A. Hansen, T. F. Jaramillo, J. Rossmeisl, I. Chorkendorff, J. K. Nørskov, *Nat. Chem.* **2009**, *1*, 552–556; c) F. J. Lai, H. L. Chou, L. S. Sarma, D. Y. Wang, Y. C. Lin, J. F. Lee, B. J. Hwang, C. C. Chen, *Nanoscale* **2010**, *2*, 573–581; d) X. Huang, Z. Zhao, L. Cao, Y. Chen, E. Zhu, Z. Lin, M. Li, A. Yan, A. Zettl, Y. M. Wang, *Science* **2015**, *348*, 1230–1234; e) L. Zhang, S. Yu, J. Zhang, J. Gong, *Chem. Sci.* **2016**, *7*, 3500–3505.

[3] a) J. Zhang, M. B. Vukmirovic, Y. Xu, M. Mavrikakis, R. R. Adzic, *Angew. Chem. Int. Ed.* **2005**, *44*, 2132–2135; *Angew. Chem.* **2005**, *117*, 2170–2173; b) J. Zhang, F. H. B. Lima, M. H. Shao, K. Sasaki, J. X. Wang, J. Hanson, R. R. Adzic, *J. Phys. Chem. B* **2005**, *109*, 22701–22704; c) R. R. Adzic, J. Zhang, K. Sasaki, M. B. Vukmirovic, M. Shao, J. X. Wang, A. U. Nilekar, M. Mavrikakis, J. A. Valerio, F. Uribe, *Top. Catal.* **2007**, *46*, 249–262; d) J. X. Wang, H. Inada, L. Wu, Y. Zhu, Y. Choi, P. Liu, W.-P. Zhou, R. R. Adzic, *J. Am. Chem. Soc.* **2009**, *131*, 17298–17302; e) C. Koenigsmann, A. C. Santulli, K. Gong, M. B. Vukmirovic, W. P. Zhou, E. Sutter, S. S. Wong, R. R. Adzic, *J. Am. Chem. Soc.* **2011**, *133*, 9783–9795; f) L. Yang, M. B. Vukmirovic, D. Su, K. Sasaki, J. A. Herron, M. Mavrikakis, S. Liao, R. R. Adzic, *J. Phys. Chem. C* **2013**, *117*, 1748–1753; g) X. Tian, J. Luo, H. Nan, H. Zou, R. Chen, T. Shu, X. Li, Y. Li, H. Song, S. Liao, R. R. Adzic, *J. Am. Chem. Soc.* **2016**, *138*, 1575–1583; h) K. Sasaki, H. Naohara, Y. Cai, Y. M. Choi, P. Liu, M. B. Vukmirovic, J. X. Wang, R. R. Adzic, *Angew. Chem. Int. Ed.* **2010**, *49*, 8602–8607; *Angew. Chem.* **2010**, *122*, 8784–8789.

[4] a) K. Gong, F. Du, Z. Xia, M. Durstock, L. Dai, *Science* **2009**, *323*, 760–764; b) Y. Yao, B. Zhang, J. Shi, Q. Yang, *ACS Appl. Mater. Interfaces* **2015**, *7*, 7413–7420; c) H. Peng, S. Hou, D. Dang, B. Zhang, F. Liu, R. Zheng, F. Luo, H. Song, P. Huang, S. Liao, *Appl. Catal. B* **2014**, *158–159*, 60–69; d) H. Peng, Z. Mo, S. Liao, H. Liang, L. Yang, F. Luo, H. Song, Y. Zhong, B. Zhang, *Sci. Rep.* **2013**, *3*, 1765; e) K. Wan, Z.-p. Yu, X.-h. Li, M.-y. Liu, G. Yang, J.-h. Piao, Z.-x. Liang, *ACS Catal.* **2015**, *5*, 4325–4332; f) K. Wan, G.-F. Long, M.-Y. Liu, L. Du, Z.-X. Liang, P. Tsiakaras, *Appl. Catal. B* **2015**, *165*, 566–571.

[5] a) I. K. Konstantinou, T. A. Albanis, *Appl. Catal. B* **2004**, *49*, 1–14; b) A. Houas, H. Lachheb, M. Ksibi, E. Elaloui, C. Guillard, J. M. Herrmann, *Appl. Catal. B* **2001**, *31*, 145–157; c) R. Li, X. Tao, R. Chen, F. Fan, C. Li, *Chem. Eur. J.* **2015**, *21*, 14337–14341.

[6] B. Kolodziejczyk, O. Winther-Jensen, D. R. MacFarlane, B. Winther-Jensen, *J. Mater. Chem.* **2012**, *22*, 10821.

[7] a) L. Zhang, L. Bai, M. Xu, L. Han, S. Dong, *Nano Energy* **2015**, *11*, 48–55; b) L. Zhang, Z. Xu, B. Lou, L. Han, X. Zhang, S. Dong, *ChemSusChem* **2014**, *7*, 2427–2431.

[8] a) B. C. Thompson, J. M. Frechet, *Angew. Chem. Int. Ed.* **2008**, *47*, 58–77; *Angew. Chem.* **2008**, *120*, 62–82; b) J. Wang, F. Zhang, M. Zhang, W. Wang, Q. An, L. Li, Q. Sun, W. Tang, J. Zhang, *Phys. Chem. Chem. Phys.* **2015**, *17*, 9835–9840; c) S. Guenes, H. Neugebauer, N. S. Sariciftci, *Chem. Rev.* **2007**, *107*, 1324–1338; d) L. Ye, W. Jiang, W. Zhao, S. Zhang, Y. Cui, Z. Wang, J. Hou, *Org. Electron.* **2015**, *17*, 295–303; e) G. Zhao, Y. He, Y. Li, *Adv. Mater.* **2010**, *22*, 4355–4358.

Received: July 22, 2016
Revised: August 24, 2016
Published online: October 20, 2016

